PREDICTION OF FORMING LIMITS OF TUBE HYDROFORMING PROCESS - SIMULATION AND EXPERIMENTS

Roberto Bortolussi[*], Sergio Tonini Button[**]

[*]*Dept. of Mechanical Eng., UniFEI, São Bernardo Campo - SP, 09850-901, Brazil*
[**]*Mechanical Engineering Faculty, Materials Department, State University of Campinas, Campinas - SP, 13083-970, Brazil*

ABSTRACT: Industries have been developing production methods and processes to improve the productivity and reduce costs of parts, assemblies and products. The hydroforming process is one of these processes that are being used with this objective, especially for the automotive and auto-parts industries, to manufacture body, motor and suspension parts. In this investigation a tool set to produce "T" parts was designed and manufactured, and instrumented to monitor the process. Tubular parts were hydroformed with these tools and the values of internal pressure and deformation load as a function of punch displacement were measured. The tube hydroforming process was simulated using the finite element method with explicit formulation. In the material model used in the simulations the anisotropy of tube steel were considered. The values of internal pressure as a function of punch displacement were input in the finite element model to get the displacements of the tube, the component stresses in the elements, and the effective strain. The effective strain was compared with the forming limit that has been proposed by Asnafi. In the simulation, the effective strain calculated was 0.35 in the stretching region and the limit calculated using the forming limit was 0.33. During the experiments the tube fractured at the same time of the simulations. The deformation load obtained in the simulation was compared with the experimental deformation load. The behavior of the load in the simulations and experiments was similar. The deformation load has two different paths during de process. First, while the tube does not yield, the deformation load has a strong increase for little displacements of the tube and after the yield when the displacements are big for little load increase.

1. INTRODUCTION

Industries, mainly automotive industries, have been looking for new processes to reduce the production costs and the time to the development of new products with low-weight. One of these new processes is the tube hydroforming. The development of this process for automotive industries is relative new and many process variables have been studied, like: friction, material properties, pressures and displacement path during the process. The simulation is a very important method to help to develop this process. Using finite element method many researches have been studying the influence of these variables in the process and they are applying forming limit expressions to define whether the material will resist to the deformation or not.

In this work using finite element method of explicit formulation, the tube hydroforming process of low-carbon steel of “T” branch was simulated to determine displacements, strain, stresses and load during the deformation process. The equivalent strain obtained in the simulation was compared with the limit equivalent deformation for anisotropic materials proposed by Asnafi (Asnafi[1999]). Experimental results were compared with simulation results.

2. THEORETICAL BACKGROUND

2.1. Equivalent stress and strain for anisotropic materials.

Anisotropy has an important role in processes like deep drawing, hydroforming and tube hydroforming. Materials that have high anisotropic indexes can support higher tensile strains than materials with low indexes. In deep drawing high anisotropic indexes will make higher ears in the top of the cup.

For anisotropic materials the equivalent stress using the Hill criterion is (Slater[1977]):

$$2f(\sigma_{ij}) \equiv F(\sigma_y - \sigma_z)^2 + G(\sigma_z - \sigma_x)^2 + H(\sigma_x - \sigma_y)^2 + 2L\tau_{yz}^2 + 2M\tau_{zx}^2 + 2N\tau_{xy}^2 = 1 \quad (1)$$

The strain plastic increments using de Lévy-Mises theory are:

$$d\varepsilon_x^p = dl.\{G(\sigma_x - \sigma_z) + H(\sigma_x - \sigma_y)\} \quad (2)$$

$$d\varepsilon_y^p = dl.\{F(\sigma_y - \sigma_z) + H(\sigma_y - \sigma_x)\} \quad (3)$$

$$d\varepsilon_z^p = dl.\{G(\sigma_z - \sigma_x) + F(\sigma_z - \sigma_y)\} \quad (4)$$

$$d\gamma_{yz}^p = dl\, L\tau_{yz} \quad (5)$$

$$d\gamma_{zx}^p = dl\, M\tau_{zx} \quad (6)$$

$$d\gamma_{xy}^p = dl\, N\tau_{xy} \quad (7)$$

The equivalent strain increment is defined as:

$$d\bar{\varepsilon} = \left(\frac{3}{2}\right)^{\frac{1}{2}}.(F+G+H)^{\frac{1}{2}}.\left\{F.\left[\frac{(G.d\varepsilon_y - H.d\varepsilon_z)}{(FG+GH+HF)}\right]^2 + A\right\}^{\frac{1}{2}} \quad (8)$$

$$A = 2.\left(\frac{d\gamma_{yz}^2}{L} + \frac{d\gamma_{zx}^2}{M} + \frac{d\gamma_{xy}^2}{N}\right) \quad (9)$$

2.2. Plastic instability

During tube hydroforming, the part is submitted to high pressure and the material has to support high strains, especially thickness strain, in regions that are not in contact with the die.

Thickness strain can lead to the failure of the process because of plastic instability. There are two kinds of plastic instability: diffuse and local. In this paper will be considered only the local instability.

Plastic instability can be written as:

$$\frac{d\bar{\sigma}}{d\bar{\varepsilon}} = \frac{1}{z}\bar{\sigma} \quad (10)$$

Hill[1952] apud Mahmudi[1996] proposed a function $\frac{1}{z}$ for isotropic materials. Rees[1995] using hydraulic bulge test proposed a function for anisotropic materials. With this function is possible to calculate the value of effective strain until the plastic instability.

Asnafi[1996] apud Asnafi[1999], using free bulging tube deformation, shows that equivalent strain to plastic instability can be written as:

$$\bar{\varepsilon}_f = (1+R).n \quad (11)$$

This expression will be used in this work to determine the limits of the process.

3. PRODUCT AND MATERIAL MECHANICAL PROPERTIES

The product for the experiments and simulation is shown in figure 1. It is made of SAE 1006 low-carbon steel welded tube. Table 1 shows the mechanical properties of the product material and table 2 shows the anisotropic indexes, mean and standard deviation for three specimens for three different directions in relation of rolling direction.

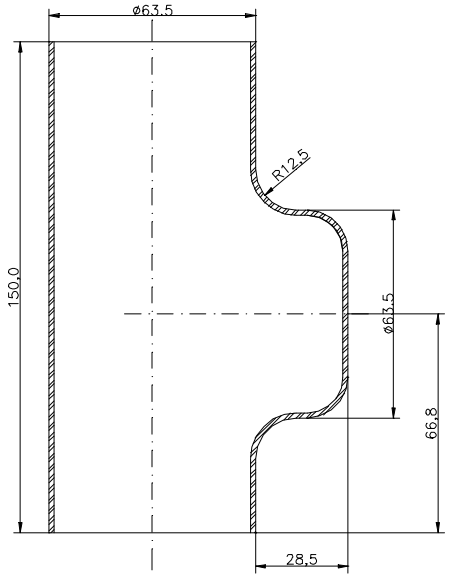

Figure 1. Product for experiments and simulation.

Table 1. Mechanical properties

Material Propriety	0°	45°	90°
Yield Stress (MPa)	321±8	331±18	292±9
Ult. Stress (MPa)	361±2	368± 2	355±1
Uniform elongation (%)	13.1±2.1	11.2±1.1	14.0±1.1
Total elongation in 50 mm (%)	34.3±1.2	31.7±2.1	35.3±2.0

Table 2. Anisotropic indexes

Direction	0°	45°	90°
Index	1.39±0.08	1.12±0.09	1.23±0.06

The specimens for mechanical properties tests and determination of anisotropic indexes were cut directly from the tube. Because of this, the values of yield stress are bigger while the values of uniform

elongation are smaller than values normally found in the reference (Hosford and Cadell [1983]) and the values of total elongation and ultimate stress are in accordance with the references, because they were not affected by the strain hardening of material due to the deformation process for the tube production.

4. EXPERIMENTAL PROCEDURES

The tools used in the experiments are shown in the figure 3 and are shown assembled in the hydraulic press is in figure 4.

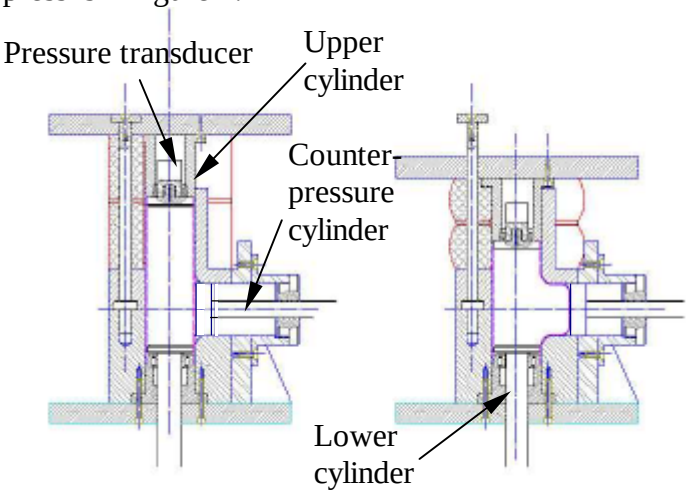

Figure 3. Tube hydroforming tools. A – initial position (without deformation). B – final position.

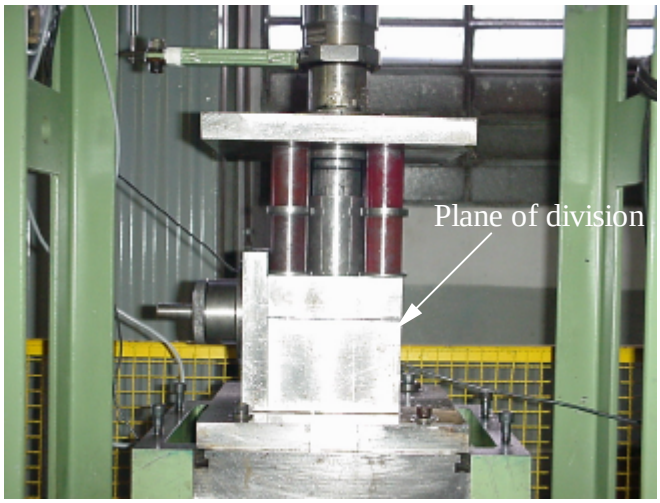

Figure 4. Hydroforming tools in the hydraulic press.

The die is separated in the center. For the experiments the specimen is put into the lower part of the die. The pressure medium is put inside of the tube and the die is closed to verify if there is no leaking. The tube for experiments had length of 189.5 mm. In this experimental apparatus there is no external pressure unit and the internal pressure is generate by the displacement of the top of tube. Pressure can be increased using the lower cylinder. Only the upper cylinder moves the tube end.

The product is shown in figure 5.

Figure 5. Product obtained in the experiments.

During the compression the internal pressure increased as shown in figure 6 and it was measured with a pressure transducer shown in figure 3 in four different tests.

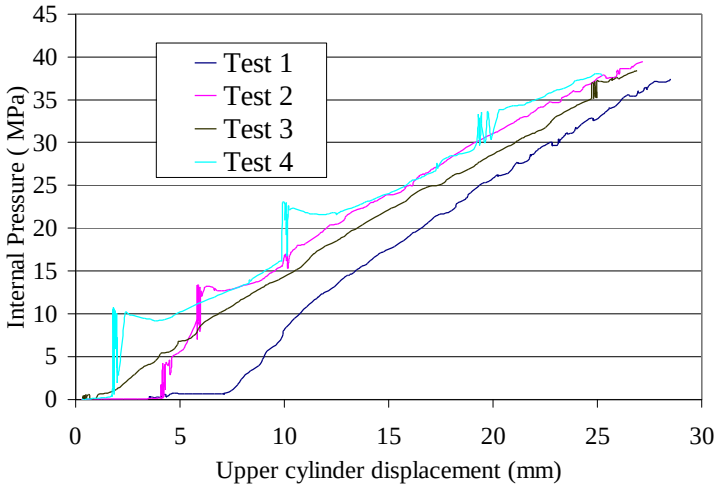

Figure 6. Internal pressure as a function of upper cylinder displacement.

The pressure has a linear behavior with the punch displacement. In the test 4, the lower cylinder was used so the values had a variation when compared with the others tests.

Four tests were taken and all tests failed during the process. Table 3 shows the final dimension of the specimens and figure 7 shows the aspect and position of the failure in the product.

The fracture begins in the intersection of plane region of the surface of dome with the free bulge region, i.e. in the region of the radius. Using

expression (11) the effective strain calculated to the fracture is 0.33. The value of anisotropic index used in the expression is the mean value among of the three directions, assumed because the value of anisotropic indexes are close.

Table 3. Final dimensions of products

Test	Final length (mm)	Bulge height (mm)
1	162.20	20.30
2	163.30	22.30
3	161.20	23.40
4	165.10	22.80
	162.95±1.67	22.20±1.34

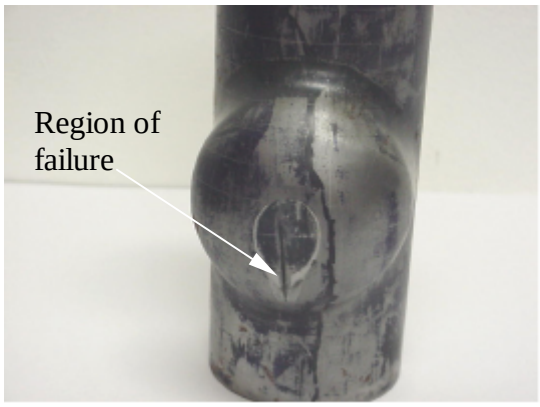

Figure 7. Aspect of the fracture

The deformation load is shown in figure 8. It was obtained with a pressure transducer in a hydraulic circuit of the upper cylinder of the press.

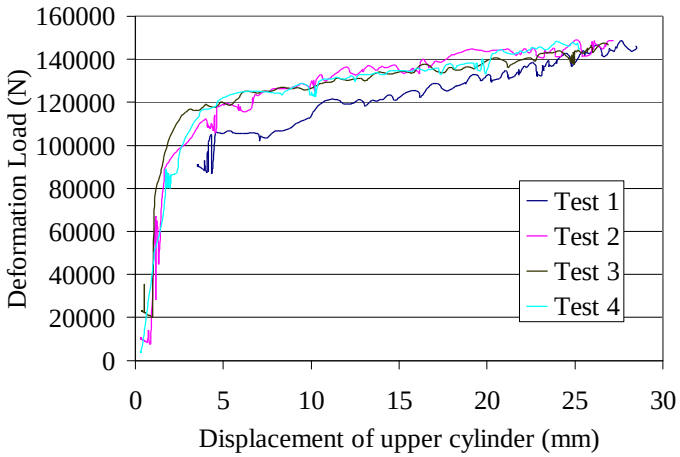

Figure 8. Deformation load

There are two different paths for the deformation load. First deformation load increased until initial flow of the central part of the tube. After this, the load increased with smaller rate than until the end of each test.

5. FINITE ELEMENT

5.1. Model

For simulation it was used MSC/Patran® as pre and post processor and MSC/Dytran® as solver. Due to product symmetry only one half of the die and tube was modeled. Die and cylinders were modeled with 3112 rigid elements and the tube was modeled with 2015 BLT elements. The model is shown in figure 9.

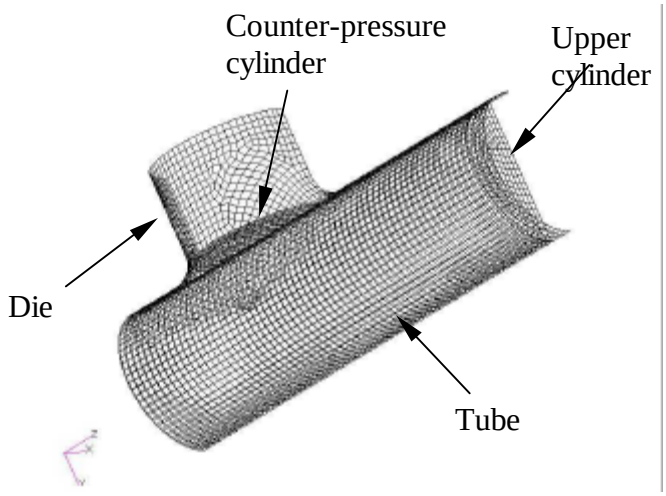

Figure 9. Finite element model.

5.2. Material model

Tube material was modeled as an elasto-plastic anisotropic material. This model is described in Krieg and Brown[1996]. Power law of this model is shown bellow and the values used are in table 4.

$$s = \left[A + K\left(\varepsilon_0 + \varepsilon\right)^n + \left(1 + C\dot{\varepsilon}^m\right)\right] \qquad (12)$$

Table 4. Values used in expression (12)

Terms	Value
Stress constant (A)	0
Strength constant (K)	535
Initial deformation (ε_0)	0.016
Strain hardening exponent (n)	0.15

Strain rate effects were not considered because the process velocity was low.

5.3. Loads

The model has three different loads. Upper cylinder had a displacement of 26.5 mm, internal pressure

increased 1.407 MPa for each millimeter of displacement of upper cylinder and counter-pressure load increased 340 N for each millimeter of displacement of upper cylinder.

5.4. Friction

Friction was modeled using Coulomb friction law. Two different friction coefficients were used. For the contact between tube and die the value was 0.05 and for contact between upper cylinder and tube and counter-pressure cylinder and tube was used 0.15 (Mac Donald and Hashmi, [2000]).

6. RESULTS

6.1. Displacements

Figure 10 shows deformed tube that is similar to the shape shown in figure 6. The displacement of dome of deformed region was 22.7 mm.

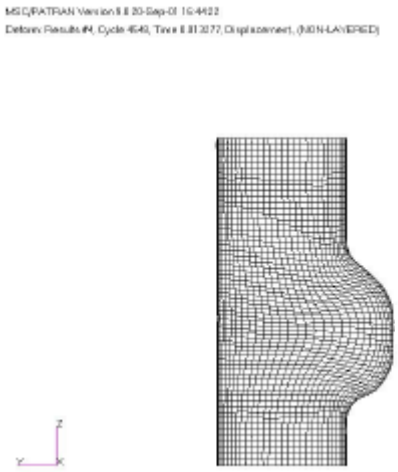

Figure 10. Deformed tube.

Effective plastic strain distribution is shown in figure 11. In this distribution shows two important regions: first in the center of the tube where are the biggest values of effective strain, but the failure does not occur in this point because compressive strain is predominant.

In the frontal part of the tube effective strain is smaller than in the center but tensile strain is predominant, so this region is where failure occurs. Another important aspect is the radius region bellow the plane part in the tube. It has a similar behavior of biaxial stretching. Values of stress in *x* and *y* directions of element coordinate system are in figure 12 and 13. The value of effective strain in this region is 0.35, close to that calculated using expression (11).

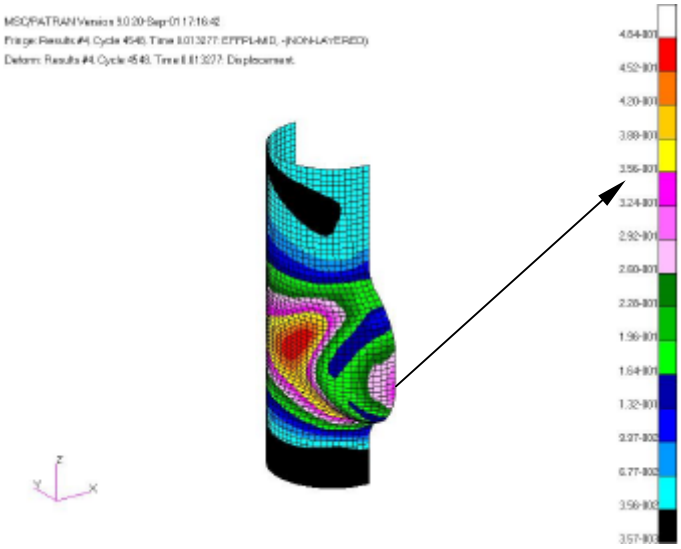

Figure 11. Effective strain distribuiton

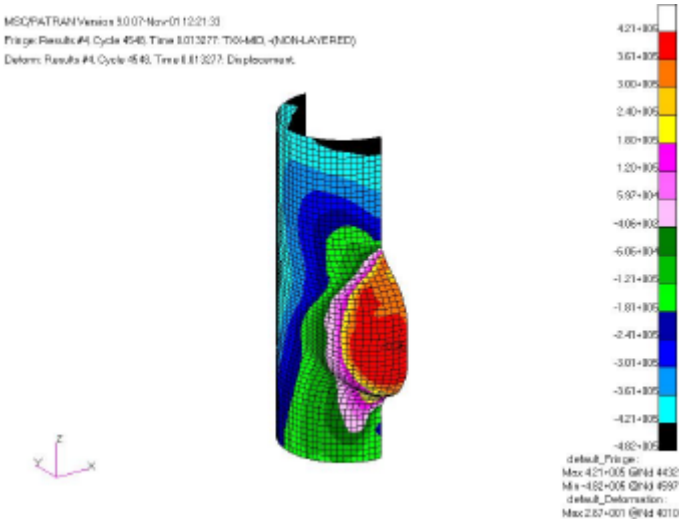

Figure 12. Stress in *x* direction of element coordinate system (values in kPa).

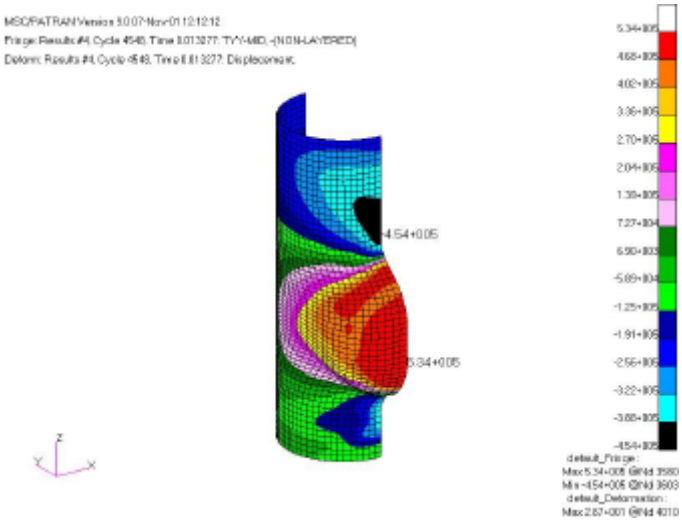

Figure 13. Stress in *y* direction of element coordinate system (values in kPa).

Deformation load is shown in figure 14. Simulation

results have the same aspect of experiments results. Difference in values of tests and simulation can be attributed to variations of the friction coefficient and oscillations of internal pressure during the tests.

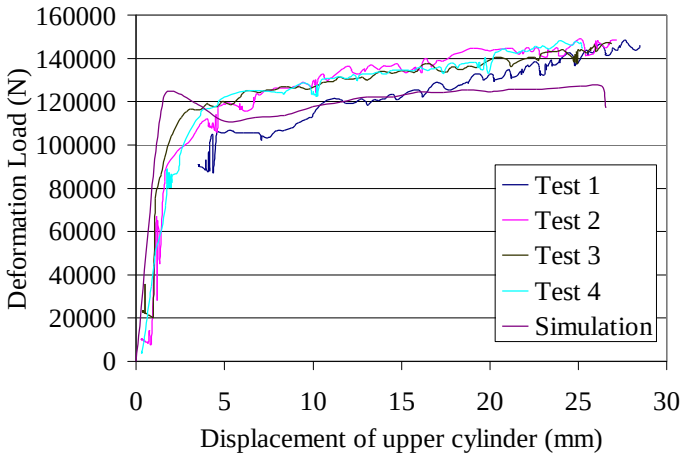

Figure 14. Deformation load tests and simulation.

5. CONCLUSIONS

Parts in “T” form were made and the process was simulated using finite element method. A tooling set was designed for the process and parts were formed without an external pressure unit. This process has the problem that is impossible to control of pressure during the operation.

The material of the tube was modeled anisotropic effects.

The expression proposed by Asnafi, in this case, showed good results to determine the deformation limits for hydroforming parts. Results of simulation are in accordance with the experimental results. The load of deformation obtained in simulation is very close to that obtained in the experiments.

REFERENCES

[1] Asnafi, 1999, Asnafi, N., " Analytical modeling of tube hydroforming ", Thin-Walled Structures, vol. 34, 295-330.

[2] Slater, 1977, Slater, R. A. C., " Engineering Plasticity ", 1st Edition, The Macmillan Press, 1977.

[3] Mahmudi, 1996, Mahmudi, R., " Plastic instability in equi-biaxial deformation of aluminum alloy sheet ", Journal of Materials Processing Technology, vol. 57, 266-271, 1996.

[4] Rees, 1995, Rees, D. W. A., " Instability limits to the forming of sheet metals ", Journal of Materials Processing Technology, vol. 55, 146-153, 1995.

[5] Hosford e Caddell, 1993, Hosford, W. F., Caddell, R. M., " Metal Forming ", 2nd edition, Prentice Hall, 1993.

[6] Krieg e Brown, 1996, Krieg, R., Brown, K. H., " Anisotropic plasticity with anisotropic hardening and rate dependence ", Journal of Engineering Mechanics, vol. 122, nº 4, 316-324, 1996.

[7] Mac Donald e Hashmi, 2000, Mac Donald, B. J., Hashmi, M. S. J., " Finite element simulation of bulge forming of a cross-joint from a tubular blank ", Journal of Materials Processing Technology, vol. 103, 333-342, 2000.

[8] Ahmetoglu e Altan, 2000, Ahmetoglou, M., Altan, T., " Tube hydroforming: state-of-the-art and future trends ", Journal of Materials Processing Technology, vol. 98, 25-33, 2000.

[9] Koç e Altan, 2001, Koç, M., Altan, T., " An overall review of the tube hydroforming (THF) technology, Journal of Materials Processing Technology, vol. 108, 384-393, 2001.

[10] Koç et al, 2001, Koç, M., Yingyot, A., Altan, T., " On the characteristics of tubular materials for hydroforming - experimentation and analysis ", International Journal of Machine Tools & Manufacture, vol. 41, 761-772, 2001.

[11] Dohmann e Hartl, 1996, Dohmann, F., Hartl, C., " Hydroforming - a method to manufacture light-weight parts", Journal of Materials Processing Technology, vol. 60, 669-676, 1996.